

Scheme S1 Chemicals and materials

Cobalt nitrate hexahydrate ($\text{Co}(\text{NO}_3)_2 \cdot 6\text{H}_2\text{O}$, 99%), sodium hydroxide (NaOH, 96%), ethylenediaminetetraacetic acid ($\text{C}_{10}\text{H}_{16}\text{N}_2\text{O}_8$, 99.5%), hydrazine hydrate ($\text{N}_2\text{H}_4 \cdot \text{H}_2\text{O}$, 85%), monolayer graphene oxide (GO, 95%), sodium selenite (Na_2SeO_3 , 98%), nickel foam (NF, 99.99%) Potassium hydroxide (KOH, 85%), anhydrous ethanol ($\text{CH}_3\text{CH}_2\text{OH}$, 99.7%), 2-Methylimidazole (2-methylimidazole, 98%), all the above reagents are of analytical grade.

Scheme S2 Materials characterization

The surface morphological features of the catalyst were examined using a Zeiss thermal field scanning electron microscope (SEM, GeminiSEM 300). The morphology and lattice spacing of the samples were examined using transmission electron microscopy (TEM, FEI Talos F200X), while elemental analysis was conducted via TEM-EDX (energy-dispersive X-ray spectrometer). The crystal phase of the samples was identified by a Shimadzu X-ray diffractometer (XRD, XRD-7000), while the elemental state was characterized by X-ray photoelectron spectroscopy (XPS, Thermo Scientific ESCALAB 250Xi, USA). The chemical bonds and functional groups of the samples were detected using a confocal microscopic imaging Raman spectrometer (inVia Qontor).

Scheme S3 Electrochemical tests

Electrochemical characterization tests were conducted at room temperature (25 °C) using an electrochemical workstation (CS2350M) in a 1.0M /L KOH solution (pH = 14). The experimental setup is a three-electrode system. The catalyst sample prepared by the above experimental scheme is used as the working electrode, the platinum electrode as the standard electrode, and Hg/ HgO as the reference electrode. The size of the test sample is 1.5 cm², and the working electrode is activated by 80-cycle voltammetry (CV) scanning at a scanning rate of 100 mV s⁻¹. The working electrode was tested by linear scanning voltammetry (LSV) at a scanning rate of 1 mV s⁻¹ to record the current-voltage curve. Electrochemical impedance spectroscopy (EIS) is formed with an alternating voltage amplitude of 5 mV within the frequency range of 0.1 to 100,000 Hz. Using the Nernst equation, all potential values in the experimental data corrected with respect to the reversible hydrogen electrode (RHE) are expressed as:

$$\text{Evs.RHE} = \text{Evs.Hg/HgO} + 0.0977 + 0.0592 \text{ pH}$$

The electrochemical surface area (ECSA) of the sample was obtained by conducting cyclic voltammetry tests on the sample at different scanning rates and calculating the double-layer capacitance (Cdl) of the sample based on the obtained results. The conversion frequency (TOF) of the sample is calculated based on

$$\text{TOF} = jS/4 nF$$

Where S, j, n and F represent the electrode surface area, current density, amount of substance and Faraday constant (96485 C mol⁻¹), respectively. The constant current polarization test of the sample was conducted at a current density of 10mA cm⁻² to determine the stability of the catalyst. The experimental data were obtained by averaging the results of three separate tests conducted on the same sample.

Scheme S4 Theoretical calculation details

This research is based on Density Functional Theory (DFT). The density of states and adsorption behavior of CoSe₂/ graphene heterostructures were systematically calculated and analyzed using the Vienna Ab initio Simulation Package (VASP) program. The exchange-correlation energy terms are presented in the form of the Perdew-Burke-Ernzerhof (PBE) function in the generalized gradient approximation (GGA). The ion-electron interaction is described by the projected add-on pseudopotential (PAW) method. The electron wave function is expanded by plane waves, and the truncation energy of the plane waves is set to 500 eV. The convergence criterion for geometric optimization of the system is set as the force on atoms being less than 0.02 eV/ Å. The electronic convergence accuracy is set at 1×10⁻⁶ eV. The Fermi surface is processed using the Gaussian broadening method, and the broadening factor is 0.05 eV. Meanwhile, to ensure the accuracy of the Brillouin zone integral, the sampling at point K adopts the Monkhorst-Pack method and is set as 5×2×1 along the x, y, and z directions respectively.

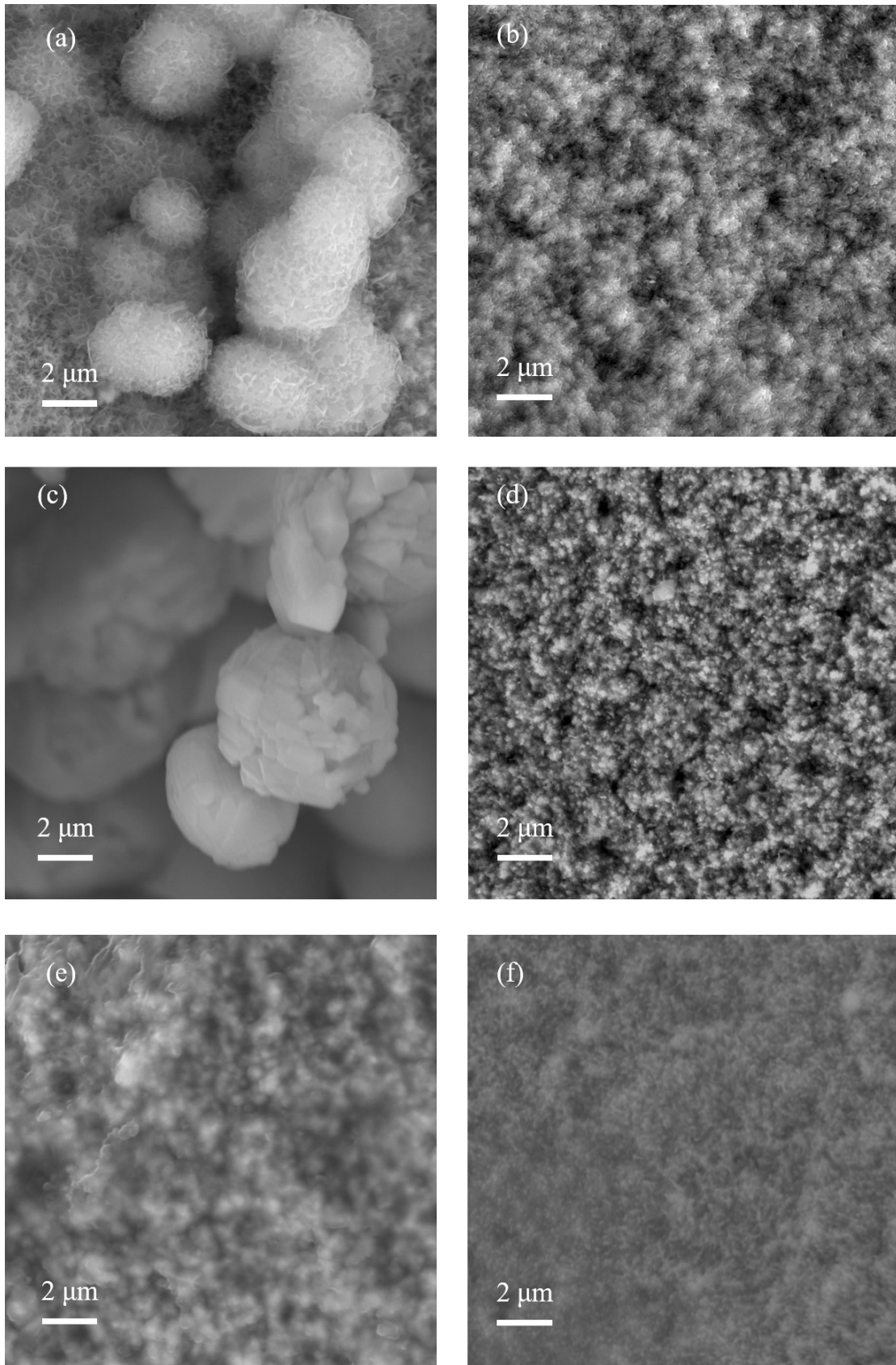


Figure S1 (a-f) SEM image of Z-N-rGO/CoSe_{2-x}N_x/NF-0, Z-N-rGO/CoSe_{2-x}N_x/NF-100, N-rGO/NiSe_{2-x}N_x/NF-0, N-rGO/NiSe_{2-x}N_x/NF-100, N-rGO/Co_{0.75}Ni_{0.25}Se_{2-x}N_x/NF-100

$x\text{N}_x/\text{NF-100}$ and $\text{N-rGO}/\text{Co}_{0.25}\text{Ni}_{0.75}\text{Se}_{2-x}\text{N}_x/\text{NF-100}$ in 5k.

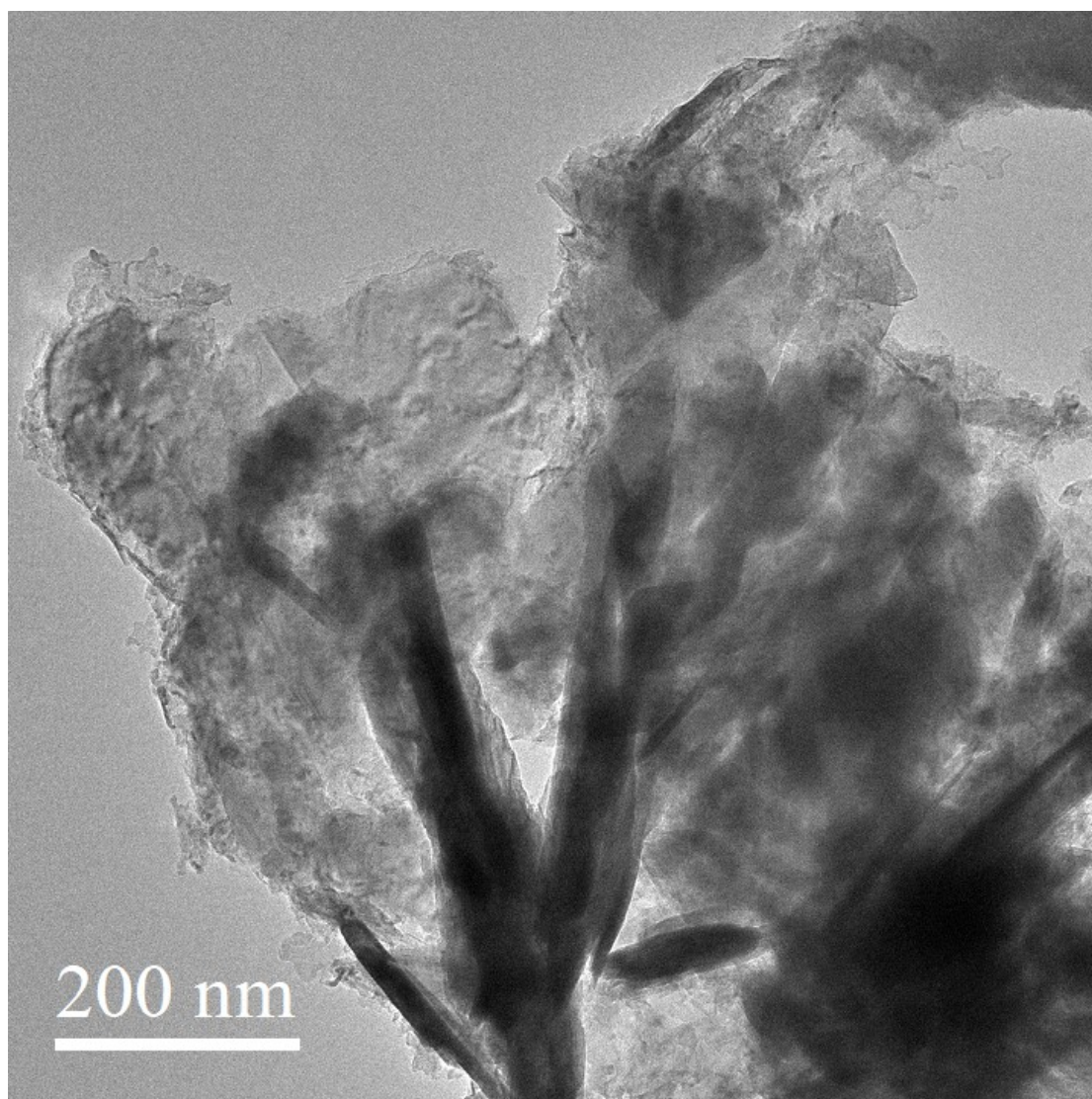


Figure S2 TEM image of $\text{N-rGO}/\text{Co}_{0.5}\text{Ni}_{0.5}\text{Se}_{2-x}\text{N}_x/\text{NF-100}$.

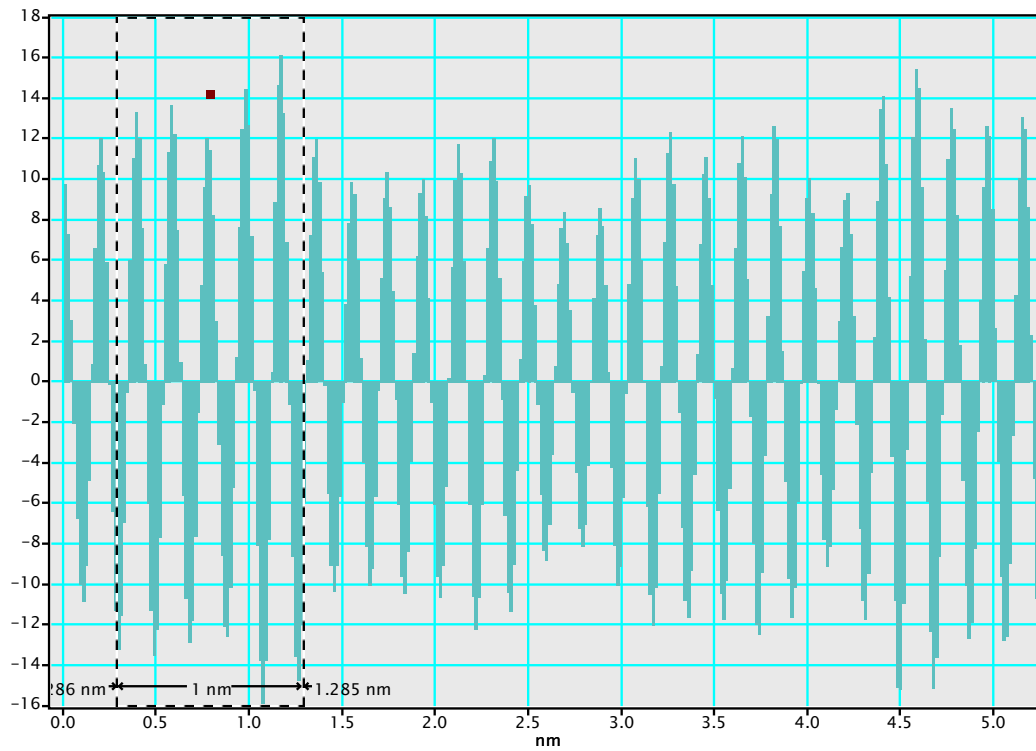


Figure S3 Calculation diagram of nickel lattice fringe spacing in N-rGO/Co_{0.5}Ni_{0.5}Se_{2-x}N_x/NF-100.

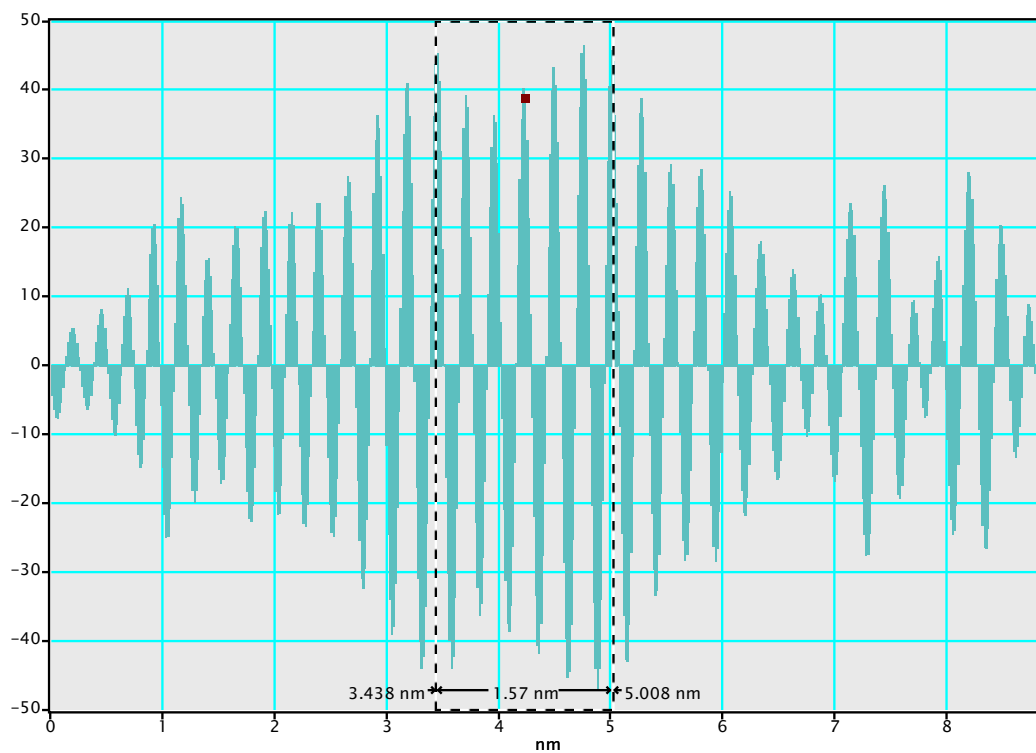


Figure S4 Calculation diagram of lattice fringe spacing of CoSe₂ in N-rGO/Co_{0.5}Ni_{0.5}Se_{2-x}N_x/NF-100.

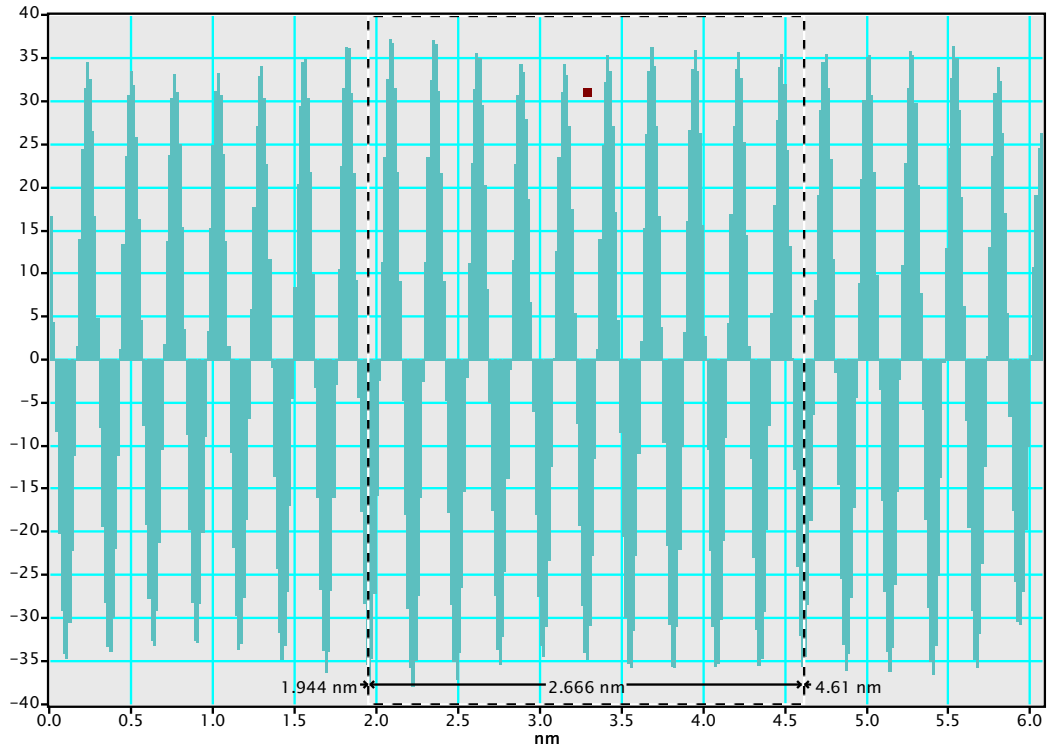


Figure S5 Calculation diagram of lattice fringe spacing of NiSe₂ in N-rGO/Co_{0.5}Ni_{0.5}Se_{2-x}N_x/NF-100.

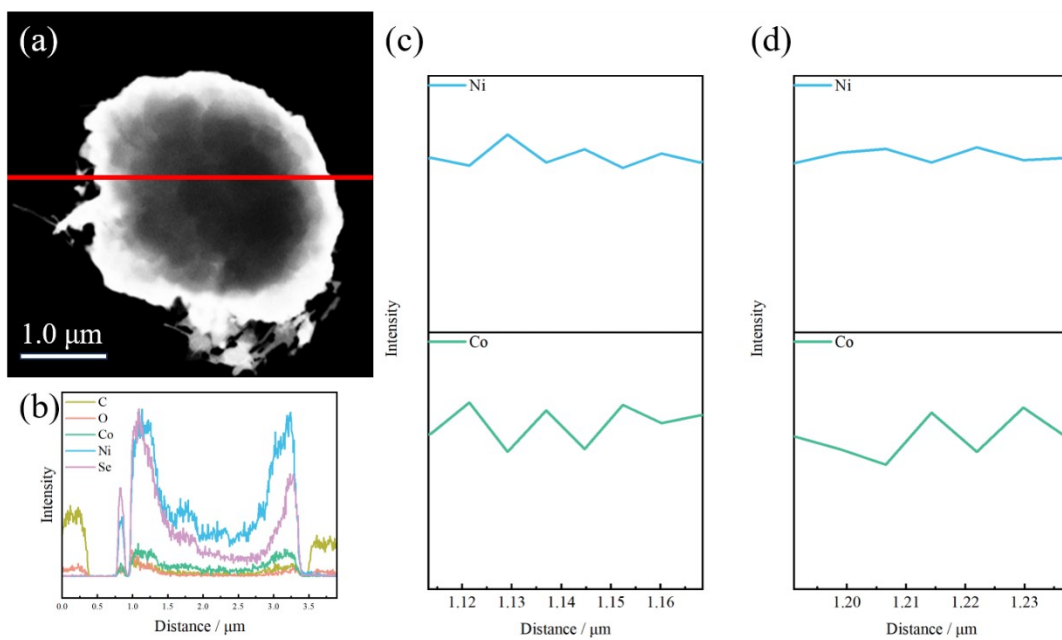


Figure S6 TEMEDS line scan results: (a) The morphology of the sample; (b) The overall results of the line-scanning data; (c, d) The selected sections from the line-scanning data results.

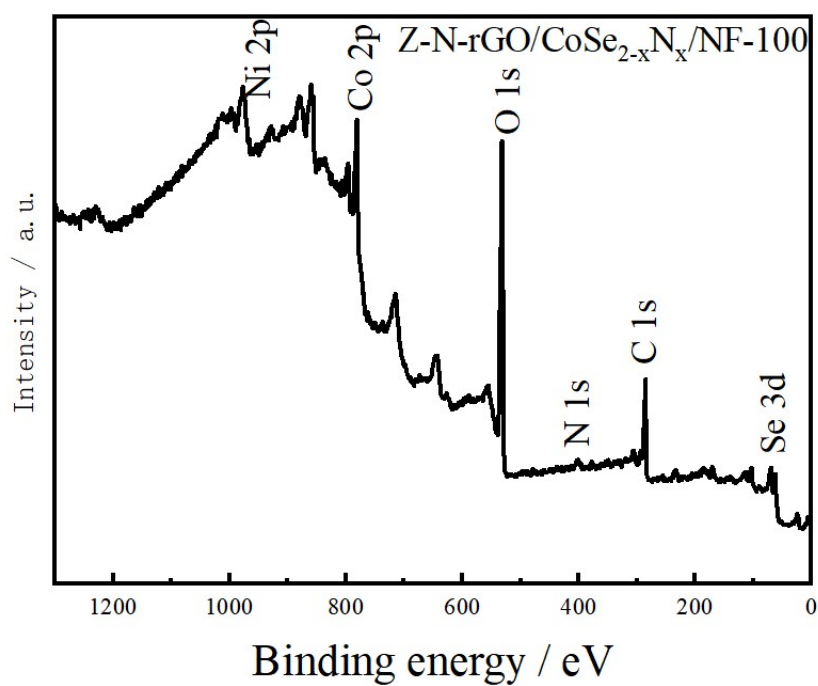


Figure S7 The total XPS measurement spectrum of Z-N-rGO/CoSe_{2-x}N_x/NF-100.

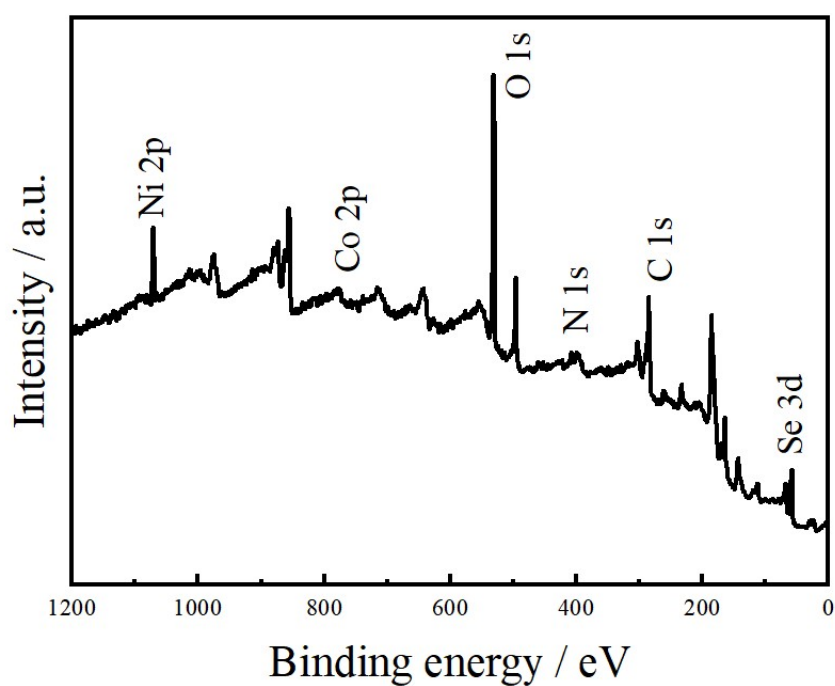


Figure S8 The total XPS measurement spectrum of N-rGO/NiSe_{2-x}N_x/NF-100.

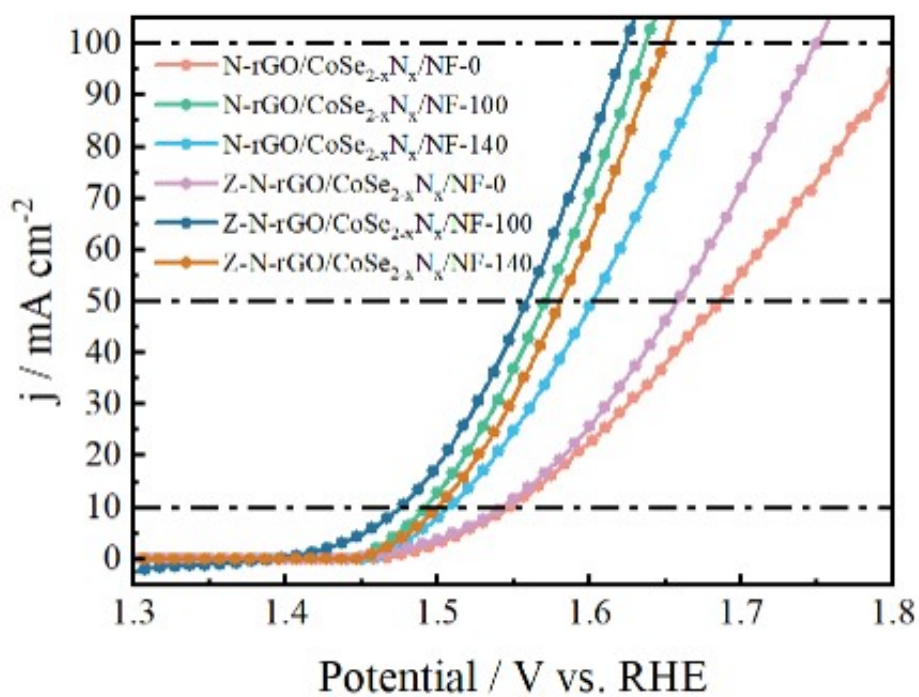


Figure S9 LSV curves of samples under different addition amounts of graphene oxide

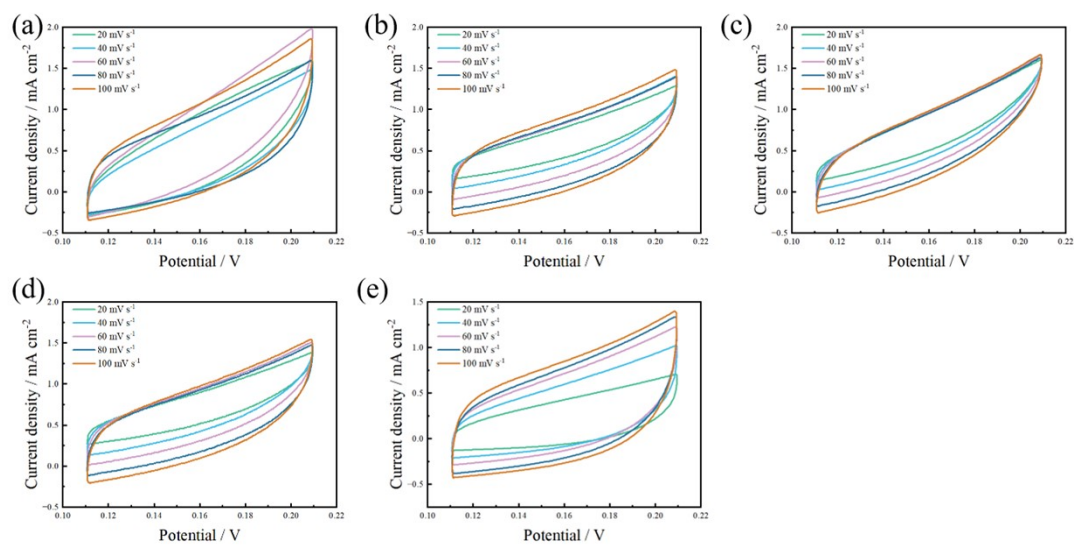


Figure S10 Cyclic voltammety curves of different samples at different scanning rates (a) N-rGO/NiSe_{2-x}N_x/NF-100; (b) N-rGO/Co_{0.25}Ni_{0.75}Se_{2-x}N_x/NF-100; (c) N-rGO/Co_{0.5}Ni_{0.5}Se_{2-x}N_x/NF-100; (d) N-rGO/Co_{0.75}Ni_{0.25}Se_{2-x}N_x/NF-100; (e) Z-N-rGO/CoSe_{2-x}N_x/NF-100.

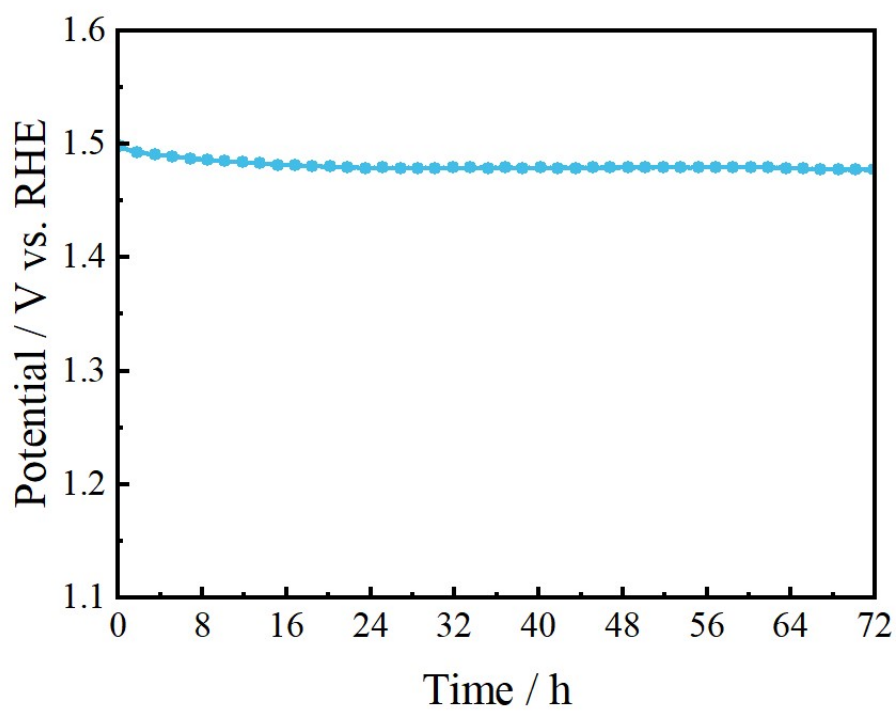


Figure S11 The stability of Z-N-rGO/CoSe_{2-x}N_x/NF-100.

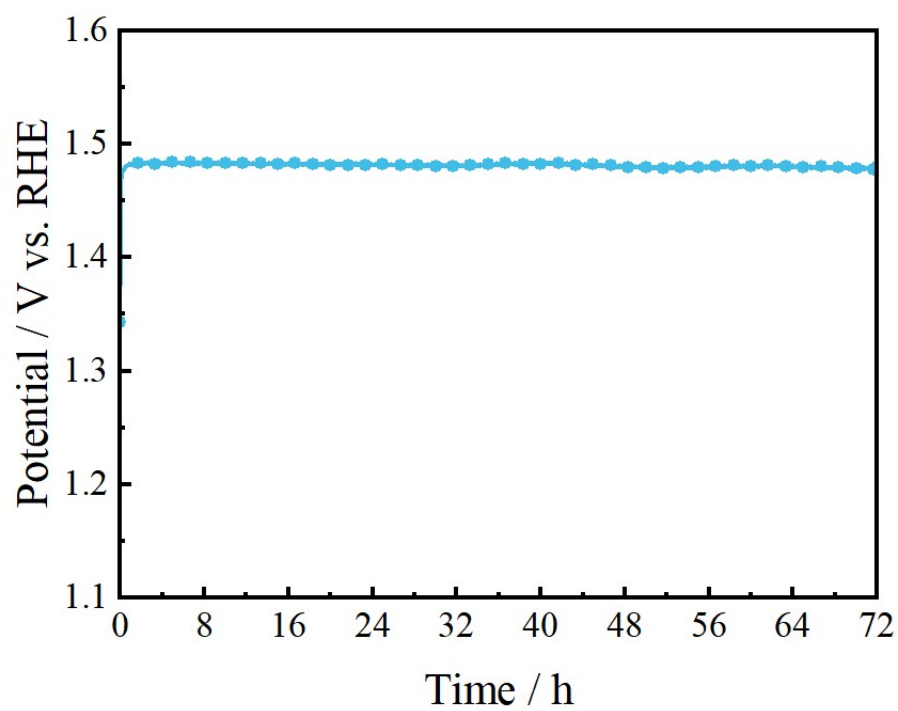


Figure S12 The stability of N-rGO/NiSe_{2-x}N_x/NF-100.

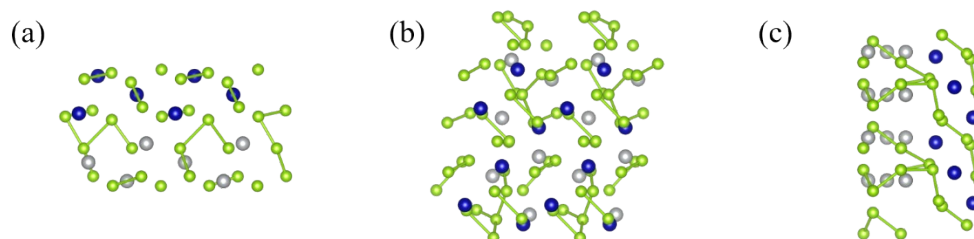


Figure S13 (a-c) Three views of the model of N-rGO/Co_{0.5}Ni_{0.5}Se_{2-x}N_x/NF-100 electrocatalyst